Colloid Polym Sci 275:672–680 (1997)

ORIGINAL CONTRIBUTION

A. Yoshino
H. Okabayashi
I. Shimizu
C.J. O'Connor

Kinetics of interaction of 3-aminopropyltriethoxysilane with silica gel using elemental analysis and ^{29}Si NMR spectra

Received: 1 November 1996
Accepted: 24 January 1997

A. Yoshino · Dr. H. Okabayashi (✉)
Department of Applied Chemistry
Nagoya Institute of Technology
Gokiso-cho
Showa-ku, Nagoya 466, Japan

I. Shimizu
Maruyasu Industries Co., Ltd.
Hashime-cho
Kitayama 1
Okazaki 444, Japan

C.J. O'Connor
Department of Chemistry
The University of Auckland
Private Bag 92019
Auckland, New Zealand

Abstract Three silica gel sample systems, modified with 3-aminopropyltriethoxy silane (APTS), were prepared by sequentially sampling the reaction mixture at various time intervals. The concentrations of 3-aminopropylsilyl groups (APS) bound on the silica surface were determined by elemental analysis. For the same sample systems, ^{29}Si NMR intensities of an $(-O)_4Si$ species belonging only to the silica gel particles and corrected by a cross-polarization correction factor were also measured. Both the APS-concentrations and the corrected ^{29}Si NMR intensities depended upon reaction time, reflecting the rate of the APTS–silica gel reaction. Kinetic analysis of these data was made by use of the Gauss–Newton method, and the overall reaction was found to consist of three reaction processes (an initial fast reaction, a slower second reaction and a much slower third reaction). In particular, the conversion of $(-O)_3SiOH$ to $(-O)_4Si$ is predominant in the second reaction process and the pore size of a silica gel particle affects the reaction mechanism.

Key words 3-aminopropyltriethoxy silane – silica gel – interaction – kinetics

Introduction

The nature of the surface of silica gel and of its interactions with various organosilane compounds has been studied intensively [1–7]. One of the most commonly used silane-modified substrates is silica gel coated with 3-aminopropyltriethoxy silane (APTS, $(CH_3CH_2O)_3SiCH_2CH_2CH_2NH_2$), which has been investigated with respect to both its reaction mechanism [5–8] and to the parameters controlling the structure of the silane-coated layer [9]. Various techniques have been applied to elucidating the modified structures. FTIR [7, 11, 12] (in particular, diffuse reflectance FTIR [13]) has proved to be a very powerful tool for characterizing the chemical structure of the silane-coated layer. Furthermore, X-ray photoelectron spectroscopy (XPS) [15], secondary ion mass spectroscopy (SIMS) [16] and atomic emission spectroscopy (AES) [17] have been successfully used for characterizing the interfacial regions.

It has already been noted that water molecules involved in the silica gel–APTS reaction system play an important role in the reaction sequence [9]. The three ethoxy groups of a silane molecule are easily hydrolyzed by water molecules, resulting in formation of SiOH groups, which can then be condensed to form a siloxane linkage between two silane molecules and generate a further water molecule which induces another condensation reaction. Therefore, the SiOH groups play a critical role in formation of modified structures on the surface of silica gel. Possible modified structures have been proposed by Vrancken et al. [10]. However, very little is known about the process for formation of a modified structure as the reaction progresses. Therefore, further investigation of the mechanism of formation of the modified structures, and in

particular, of the kinetics of interaction of silane molecules with the hydroxyl groups on the silica gel, is highly desirable.

Maciel and Sindorf [18] have indicated that the three resonance signals observed in the ^{29}Si CP/MAS spectra of silica gel can be assigned to specific Si-atom environments on the surface, thereby making possible a variety of interesting studies into the structure of silica gel. Sindorf and Maciel [19] have reported a ^{29}Si NMR study of dehydrated and rehydrated silica gel, using cross-polarization and magic-angle spinning (CP/MAS) techniques.

Caravajal et al. [20] have used CP/MAS techniques involving both ^{29}Si and ^{13}C NMR to make a systematic study of APTS-modified silica gel. Their results revealed that ^{29}Si CP/MAS spectra are extremely useful for charaterizing the nature of the attachment between the APTS-derived Si atom and the silica surface. In particular, it should be noted that the ^{29}Si NMR relative intensities of the ^{29}Si atoms of the 3-aminopropylsilyl group (APS, $(XO)_3SiCH_2CH_2CH_2NH_2$), corrected by a CP correction factor, could be used to determine quantitatively the concentration of APS moieties bound on the silica surface.

In the present study, the rate constants of the APTS–silica reaction, for APTS-modified silica gel samples prepared by sampling the reaction substrate from the reactor at various time intervals, have been determined from elemental analysis and ^{29}Si NMR intensity data. In particular, the observed ^{29}Si NMR data, corrected by a CP correction factor, have been used to analyze quantitatively the distribution of ^{29}Si atoms between the APS moieties and the silica surface.

We can use the data from the elemental analysis to monitor the time dependence of the amount of APTS modified onto the surface of silica gel, while the ^{29}Si NMR spectra of these samples provide time dependent information on both the ^{29}Si content of APS bound onto the surface and the concentration of the silica gel–SiOH which participates in the condensation reaction with an APTS molecule. Consideration of both the bound-APS concentration and the ^{29}Si NMR data makes it possible to discriminate between the silica gel–APTS reaction and the condensation reaction in the bulk phase. The effects of temperature and of pore size on the APTS–silica gel reaction are also discussed.

Experimental

Materials

Super Micro Bead Silica Gel B-5 (SMBS), with a particle size distribution of $d_{10}/d_{90} = 1.5$ and average particle diameter 5 μm, was purchased from Fuji Silysia Chemical Co. SMBS particles with pore diameters $\phi = 5.5$, 8.1 and 11.6 nm were selected so as to examine the effect of pore size on the reactivity. Particle diameter and pore diameter were determined by coulter counter method [21] and mercury porosimetry [22], respectively. Surface areas (A_s) were determined by the BET method using nitrogen adsorption (a surface area of 16.2 $Å^2$ was assumed for molecular N_2): the A_s values are 498, 437 and 384 $m^2 g^{-1}$ for $\phi = 5.5$ nm, 8.1 nm and 11.6 nm, respectively. 3-Aminopropyltriethoxy silane (APTS), obtained from Shinetsu Chemical Industry Ltd., was used for the reaction with the silica gel without further purification.

SMBS–APTS reactions

The three SMBS sample systems (SI ($\phi = 5.5$ nm), SII ($\phi = 8.1$ nm) and SIII ($\phi = 11.6$ nm)) modified with APTS were prepared as follows. SMBS (40 g) was refluxed in toluene (120 ml) and then stirred at constant temperature. The temperature of the reaction mixture in the reactor was kept at 388 K for SI and at 333 K for SII and SIII. The APTS–toluene solution (0.57 $mol l^{-1}$ for SI, 0.44 $mol l^{-1}$ for SII and 0.38 $mol l^{-1}$ for SIII, the APS–concentration per unit surface area $= 3$ $\mu mol m^{-2}$ for SI, SII and SIII) was then added to the preheated SMBS–toluene mixture. In order to follow the rate of the APTS–SMBS reaction, aliquots were removed at various time intervals, and the reaction was quenched by washing the reaction mixture with methanol. Unreacted ethoxy groups in the substrate were hydrolyzed in water–methanol (1:1) solution for 2 h at room temperature and the APTS modified SMBS was again washed with methanol. The samples thus prepared were dried at 388 K under vacuum. Care was taken that the drying temperature did not go higher than 388 K and the samples were therefore assumed to be in a fully hydrated state [3].

Elemental analysis

A Yanaco-CN Coder MT 600 was used for elemental analysis of the samples. The concentration of APS bound on the silica gel was determined by analyzing the nitrogen content of samples. The errors were $\pm$ 0.3 wt%. The nitrogen content data and the C(APS) values for the SI, SII and SIII sample systems are listed in Table 1.

^{29}Si NMR measurements

^{29}Si NMR spectra were obtained on a Varian UNITY-400 spectrometer operated at 79.5 MHz at 25 °C. The ^{29}Si

Table 1 Nitrogen contents (C_N, wt%) of the SI, SII and SIII samples and concentrations (C(APS), μmol m^{-2}) of bound APS

Sample	Reaction time t (s)	C_N ($\pm$ 0.3 wt%)	C(APS) (μmol m^{-2})
SI	60	1.04	1.59
	180	1.17	1.81
	300	1.24	1.93
	600	1.32	2.06
	900	1.34	2.10
	1800	1.43	2.25
	∞	1.34[a]	2.10[a]
SII	60	0.70	1.14
	180	0.83	1.43
	300	0.90	1.56
	600	0.99	1.72
	900	1.04	1.82
	1800	1.10	1.93
	3600	1.17	2.06
	∞	1.10[a]	1.93[a]
SIII	60	1.01	2.00
	180	1.02	2.03
	300	1.05	2.09
	600	1.10	2.20
	900	1.12	2.24
	1800	1.16	2.32
	3600	1.19	2.39
	∞	1.19[a]	2.37[a]

[a] Calculated from $C(\infty) = C_1(\infty) + C_{2,3}(\infty)$.

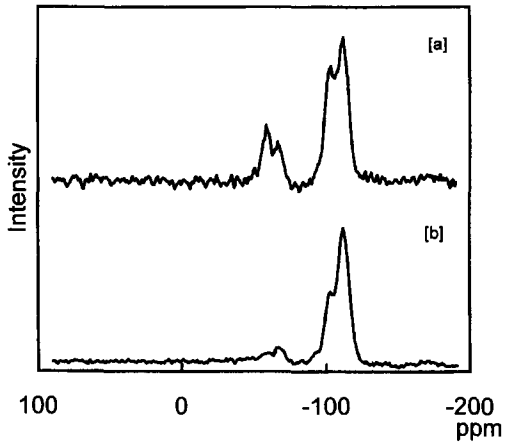

Fig. 1 ^{29}Si CP MAS ([a]) and MAS ([b]) spectra of the SI sample (reaction time: 1800 s)

Table 2 CP correction factors obtained for the SI, SII and SIII samples

	−60 ppm	−70 ppm	−100 ppm	−110 ppm
SI (1800 s)	0.47	0.92	0.96	1.96
SII (3600 s)	0.71	0.60	0.83	1.58
SII (3600 s)	0.63	0.55	0.77	2.21

chemical shifts (ppm) are given relative to external 2,2-dimethyl-2-silapentane-5-sulfonate (DSS) standard. The ^{29}Si NMR spectra were measured using an acquisition time of 0.102 s, a contact time of 2.5 ms, a recycle time of 15 s, and a pulse width of 6.3 μs. Magic angle sample spinning was routinely carried out at 4.5 kHz spinning rates. High resolution solid state ^{29}Si NMR measurements were achieved with use of a cross-polarization sequence (XPOLAR). The spectra with CP were measured by cross-polarization and magic-angle spinning (CP/MAS). The spectra without CP were measured using only MAS (designated NCP). Representative CPMAS and MAS spectra (of the SI sample, reaction time: 1800 s) are shown in Fig. 1. The two types of spectra were integrated and then the CP correction factors were obtained from division of the NCP integral values by the CP integral values for each resonance line [18]. In order to obtain the CP correction factor, MAS NMR measurements were carried out only for silica gel samples which had been condensed with APTS at the longest reaction time. The CP correction factors thus obtained (listed in Table 2) were used to correct the signal intensities of the ^{29}Si CP/MAS NMR spectra of other samples in the same sample system. This correction made it possible to discuss quantitatively the signal intensities of the ^{29}Si CP/MAS NMR spectra. Thus, the real integral values were calculated by multiplication of the CP integral values by the CP correction factors.

Results and discussion

In order to characterize the surface of silica gel which has been treated with APTS, it is important to determine the concentration of APS moieties which are chemically bonded through siloxane bonds on the surface, since the silane coating layer contains both chemically bound APS moieties and physically adsorbed silanes. In the present study, the APS-bound SMBS particles were prepared by sequentially sampling the reaction mixture at various time intervals, followed by thorough washing with methanol. Samples prepared in this way can be regarded as APS-SMBS complexes free of physically adsorbed silanes.

The ^{29}Si CP/MAS NMR spectra of the SI and SII samples are shown in Fig. 2. The two ^{29}Si resonance peaks at ca. −100 and −110 ppm are assigned to the ^{29}Si nuclei of the $(-O)_3SiOH$ and $(-O)_4Si$ species belonging to the SMBS particles, respectively [18]. The resonance peaks at ca. −90 ppm arising from geminal species $(-O)_2Si(OH)_2$ on the SMBS surface, are very weak in intensity, implying that most of the geminal OH groups were condensed with

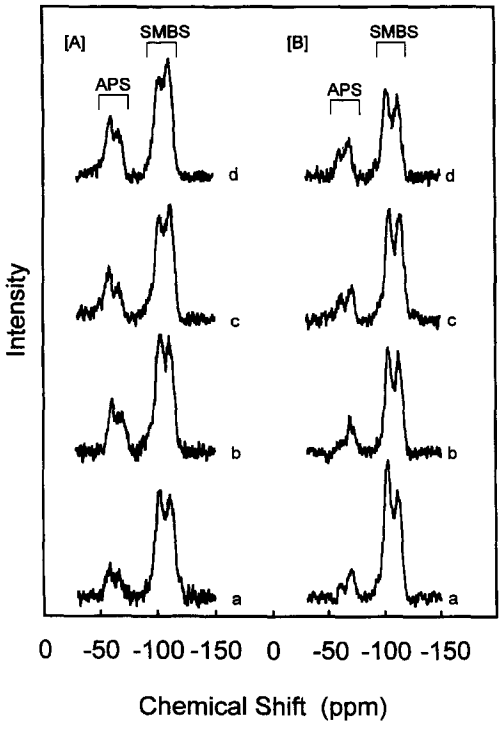

Fig. 2 ^{29}Si CP MAS NMR spectra of the SI ([A], $T = 388$ K) and SII ([B], $T = 333$ K) samples prepared at various time intervals (a: 60 s, b: 300 s, c: 1800 s and d: 21600 s)

APTS molecules. The resonance peaks at ca. -60 and -70 ppm arise from the $(-O)_2Si(OH)R$ and $(-O)_3SiR$ species, respectively, of the APS moieties bonded to the SMBS particles [20]. The spectral features of the ^{29}Si resonance peaks depend on reaction time and reaction temperature.

The ^{29}Si MAS spectra of the same samples were also measured without applying a cross-polarization sequence [18–20]. The ^{29}Si signal intensities were corrected by the CP correction factors obtained from the integrated intensities of both the CPMAS and MAS spectra [20]. The total corrected integral intensities of the three ^{29}Si signals arising only from the SMBS particles should be independent of the concentration of bound APS, while those of the three signals arising only from bound APS depend upon the concentration of APS bound on the SMBS surface. Therefore, when the total corrected integral intensities of the three ^{29}Si signals arising from the SMBS particles are arbitrarily made equal to 100, the total corrected integral intensities I(APS) of three ^{29}Si signal arising from the APS moieties can be expressed as relative corrected integral intensities (I_r(APS) [%] = [100 I(APS)]/[$I((-O)_3SiOH) + I((-O)_4Si)$]). The I_r(APS) and corrected integral intensities of the $(-O)_3SiOH$ and $(-O)_4Si$ species for SMBS ($I((-O)_3SiOH)$) and ($I((-O)_4Si)$) are listed in Table 3. The error of estimate in these values is $\pm$ 0.3%. Also shown are the values of $C((-O)_4Si)$ calculated from $I_r((-O)_4Si)$ using a proportionality constant between C(APS) and I_r(APS).

Figure 3 shows plots of relative corrected integral intensities (I_r(APS)) against the concentration of bound APS (C(APS), μmol m^{-2}). It is evident that for the three sample systems the I_r(APS) value is proportional to the concentration of bound APS moieties. It may therefore be assumed that the relative corrected integral intensities are a true reflection of the extent of reactivity of APTS with the silica gel hydroxyl moieties. Thus, the total relative corrected integral intensities directly reflect the concentration of bound APS.

Kinetic analysis of the APTS–SMBS reaction using ^{29}Si CP MAS and MAS NMR data

The relative corrected integral intensity of the ^{29}Si signal of an $(-O)_4Si$ species on the SMBS surface has been used to follow the rate of reaction, since the difference in the corrected integral intensities of the $(-O)_3SiOH$ and $(-O)_4Si$ signals is an important indicator of the reaction process.

The time dependence of the relative corrected integral intensity $I_r(t)$ of the ^{29}Si resonance signal of an $(-O)_4Si$ species is given by

$$I_r(t) = I_r(\infty) - I_r(\infty)e^{-k'(t)}, \quad (1)$$

where k' is the first-order rate constant for the $(-O)_3SiOH \rightarrow (-O)_4Si$ reaction and $I_r(\infty)$ is the relative corrected integral intensity of the ^{29}Si signal of an $(-O)_4Si$ species at $t = \infty$.

Figure 4 shows plots of the observed $I_r(t)$ values against reaction time (t) and the calculated curves of best fit for the three sample systems. The rate constants thus obtained are 6.47×10^{-3}, 3.60×10^{-3} and 1.06×10^{-3} s^{-1} for the SI, SII and SIII samples, respectively. The $I_r(\infty)$ values, determined from the curves of best fit, were equal to 77.1%, 67.2% and 72.5% for SI, SII and SIII, respectively. It should be noted that the value of the rate constant for the SI samples (6.47×10^{-3} s^{-1}) agrees well with that (6.91×10^{-3} s^{-1}) obtained from DRIFT spectral measurements [23].

Kinetic analysis of the APTS–SMBS reaction using elemental analysis data

Values of the nitrogen content of the SI, SII and SIII samples and of the concentration of APS bound on the SMBS particles (calculated from the elemental analysis

Colloid & Polymer Science, Vol. 275, No. 7 (1997)

Table 3 Relative corrected integral intensities (I_r, % ± 0.3%) of the ^{29}Si resonance lines for bound-APS, $(-O)_3SiOH$ and $(-O)_4Si$ species and the concentration (C, μmol m^{-2}) of the $(-O)_4Si$ species calculated from NMR data

	Reaction time t (s)	Corrected integral intensity I_r(%, ± 0.3%) I_r(APS)	$I_r((-O)_3SiOH)$	$I_r((-O)_4Si)$	Concentration C(μmol m^{-2})[a] $C((-O)_4Si)$
SI	0	0	38.09	62.91	9.42
	60	8.83	34.20	65.80	9.86
	180	11.89	30.46	69.54	10.42
	300	14.08	29.97	70.03	10.49
	600	13.79	28.19	71.81	10.76
	900	14.09	28.07	71.93	10.77
	1800	13.99	28.12	71.88	10.77
	∞	14.90[b]	28.10[c]	71.90[c]	10.77[c]
SII	0	0	41.31	58.69	8.90
	60	7.78	38.81	61.19	9.28
	180	8.66	35.24	64.76	9.82
	300	9.96	31.94	68.06	10.32
	600	11.60	31.42	68.58	10.40
	900	11.05	29.91	70.09	10.63
	1800	12.14	28.71	71.29	10.82
	3600	15.37	28.20	71.80	10.89
	∞	13.49[b]	28.88[c]	71.12[c]	10.79[c]
SIII	0	0	30.71	69.29	13.66
	60	10.43	30.33	69.67	13.74
	180	10.51	29.56	70.44	13.89
	300	10.71	28.69	71.31	14.06
	600	11.33	27.61	72.39	14.27
	900	11.80	27.65	72.35	14.26
	1800	11.08	25.95	74.05	14.60
	3600	11.68	24.88	75.12	14.81
	∞	12.14[b]	25.04[c]	74.96[c]	14.78[c]

[a] Calculated from $I_r((-O)_4Si)$ using a proportionality constant between C(APS) and I_r(APS).
[b] Calculated from $C(\infty)$ using a proportionality constant between C(APS) and I_r(APS).
[c] Calculated from the best fit of the calculated values to the observed $I_r(t)$ vs. t plots.

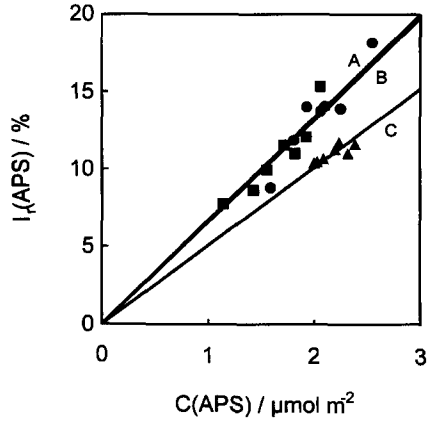

Fig. 3 Plot of I_r (APS) against C(APS) for the three sample systems (A: SI, B: SII and C: SIII)

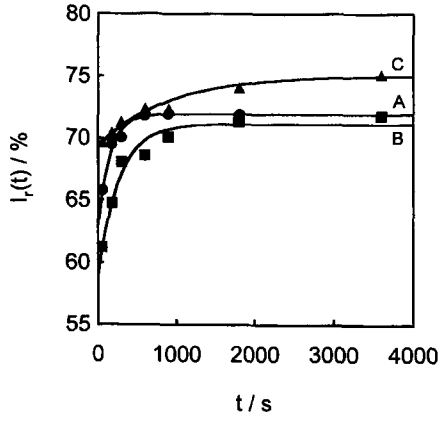

Fig. 4 Plots of $I_r(t)$ against t (●, ■ and ▲: observed) and best fit curves (solid lines) for the three sample systems (A: SI, B: SII and C: SIII)

data) are given in Table 1. The concentration of the bound-APS increases with reaction time, reflecting the rate of the APTS-SMBS reaction.

In order to interpret these elemental analysis data, it is necessary to invoke a very fast initial reaction process, followed by at least one slower process, since the time dependence of the concentration of a bound APS moiety cannot be expressed by a single exponential function. Caravajal et al. [20] have previously suggested that

polymerization of silane molecules occurs through a very fast initial reaction process.

In the present study, we have analyzed the rate data for the APTS–SMBS system, and have found that three first order reaction processes (initial, second and third processes) participate in the overall reaction. Furthermore, after 60 s of reaction time, the concentration of substrate which remains unreacted in the initial reaction process is negligibly small and will therefore not contribute to subsequent reaction processes. If we now assume that there are three reaction processes involved, we may separate the rate constants for the second and third reaction processes from the overall reaction process by using the Gauss–Newton method [24]. The time dependence of the APS-concentration ($C_{obs}(t)$) observed in the overall reaction system may be expressed by

$$C_{obs}(t) = C_1(t) + C_2(t) + C_3(t)\,, \tag{2}$$

$$C_1(t) = C_1(\infty) - C_1(\infty)e^{-k_1 t}\,, \tag{2a}$$

$$C_2(t) = C_2(\infty) - C_2(\infty)e^{-k_2 t}\,, \tag{2b}$$

$$C_3(t) = C_3(\infty) - C_3(\infty)e^{-k_3 t}\,, \tag{2c}$$

where $C_i(t)$ ($i = 1, 2$ and 3) is the APS-concentration, which depends on the reaction time (t) in the i-th reaction process, $C_i(\infty)$ denotes the APS-concentration in the i-th reaction process at $t = \infty$ and k_i ($i = 1, 2$ and 3) is the reaction rate constant in the i-th reaction process.

Since $C_1(t)$ is assumed to be approximately equal to zero during the second and third processes, Eq. (2) can then be reduced to

$$C_{obs}(t) = C_{2,3}(\infty) - C_2(\infty)e^{-k_2 t} - C_3(\infty)e^{-k_3 t}\,, \tag{3}$$

where $C_{2,3}(\infty) = C_2(\infty) + C_3(\infty)$. Equation (3) can be used to determine the values of k_2 and k_3, which provide the best fit to the $C_{obs}(t)$ data.

We may predict that the conversion of $(-O)_3SiOH$ to $(-O)_4Si$ contributes predominantly to one of the three reaction processes. In order to check this prediction, the best fit between the observed APS-concentration data and calculated values was calculated using Eq. (3) which includes five parameters ($C_{2,3}(\infty)$, $C_2(\infty)$, $C_3(\infty)$, k_2 and k_3). The calculated rate constants, k_2 and k_3, of the second and third reaction processes are listed in Table 4. The values of k_2 thus obtained (7.06×10^{-3}, 6.08×10^{-3} and $1.14 \times 10^{-3}\,s^{-1}$ for the SI, SII and SIII samples, respectively) are very similar to those calculated (Fig. 4) for the corresponding rate constants for conversion of $(-O)_3SiOH$ to $(-O)_4Si$, implying that it is this reaction which is the dominant contributor to the second reaction process. Therefore, we may assume that the $C(\infty)$ value calculated from ^{29}Si NMR intensity data ($I(\infty)$, Eq. (1)), is approximately equal to the $C_2(\infty)$ value of the second reaction process expressed by Eq. (2b).

If we now substitute values for the parameter $C_2(\infty)$, observed in the ^{29}Si NMR, and for the APS-concentration data of samples prepared at 60 s reaction time into Eq. (3), the five parameters may be reduced to only three parameters ($C_3(\infty)$, k_2 and k_3), thereby allowing us to refine the magnitude of the rate constants. Thus, kinetic analysis for all concentrations of bound APS in each sample system could also be carried out using only these three parameters.

Plots of $C_{obs}(t)$ vs. t, which provide the best fit of the calculated values to the observed data, are shown in Fig. 5 together with plots for separated curves of the second and third reactions. Values of k_2 and k_3 for the SI and SII

Fig. 5 Plots of $C_{obs}(t)$ against t (■: observed) and best fit curves (solid lines) for the SI ([A]), SII ([B]) and SIII ([C]) samples. Curves b (dashed) and c (dotted) are the second and third reaction process curves separated from the best fit curve a

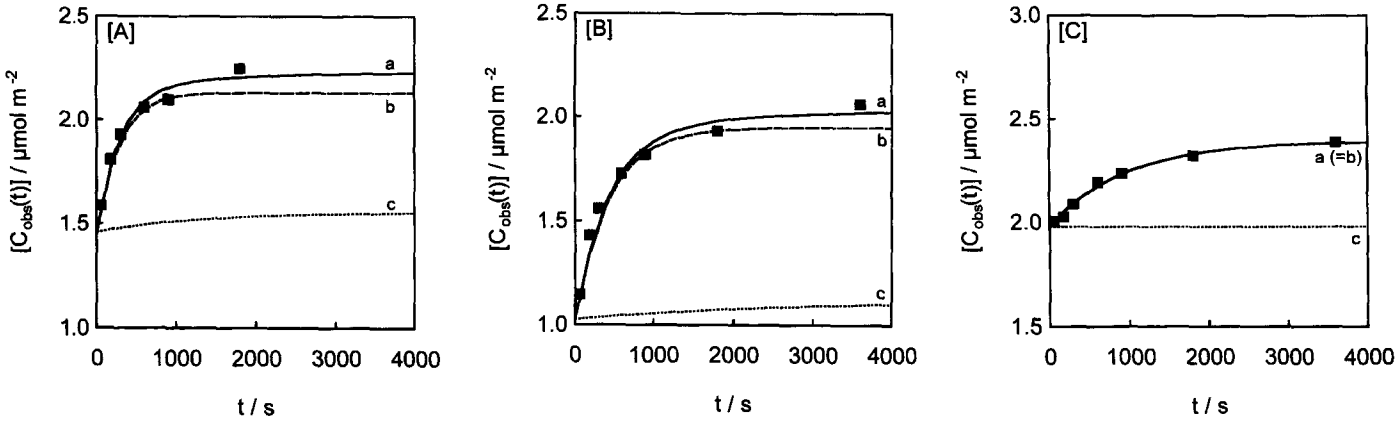

Colloid & Polymer Science, Vol. 275, No. 7 (1997)

Table 4 Kinetic parameters determined using (a) five parameters[a] and (b) three parameters[b]

		$C_2(\infty)$	k_2 (s^{-1})	$C_3(\infty)$	k_3 (s^{-1})	$C(\infty)$	$C_{2,3}(\infty)$	RMS[c]
SI	(a)	0.485	7.06×10^{-3}	0.454	8.06×10^{-4}	2.341	—	1.49×10^{-1}
	(b)	0.676	3.51×10^{-3}	0.099	7.87×10^{-4}	—	0.775	4.58×10^{-2}
SII	(a)	0.665	6.08×10^{-3}	0.110	3.47×10^{-4}	2.096	—	1.47×10^{-2}
	(b)	0.920	2.23×10^{-3}	0.097	3.47×10^{-4}	—	1.017	6.93×10^{-2}
SII	(a)	0.382	1.14×10^{-3}	0.033	9.17×10^{-4}	2.391	—	2.39×10^{-2}
	(b)	0.390	1.06×10^{-3}	—	—	—	0.390	1.74×10^{-2}

[a] $C_{2,3}(\infty)$, $C_2(\infty)$, k_2 and k_3 calculated by using Eq. (3).
[b] $C_3(\infty)$, k_2 and k_3 calculated by using Eq. (3).
[c] RMS: $[\sum_{i=1}^{n} \{C_{obs}(n) - C_{calc}(n)\}^2/(n-m)]^{1/2}$; m: the number of parameters.

sample systems and of k_2 for the SIII sample system, as obtained from the plots, are given in Table 4. The $C_{2,3}(\infty)$ values for the three sample systems were determined from both the $C_2(\infty)$ value observed in the ^{29}Si NMR analysis and the calculated value of $C_3(\infty)$. The values of the rate constant (k_1) and of $C_1(\infty)$ for the initial reaction process, which were thus obtained, are $4.14 \times 10^{-2}\ s^{-1}$ and $1.46\ \mu mol\ m^{-2}$, $3.78 \times 10^{-2}\ s^{-1}$ and $1.03\ \mu mol\ m^{-2}$, and $7.27 \times 10^{-2}\ s^{-1}$ and $1.98\ \mu mol\ m^{-2}$ for the SI, SII and SIII samples, respectively.

For both the SI and SII sample systems, in which SMBS particles with a smaller pore size were allowed to react with APTS molecules, there are significant differences in the relative rate constants for the second and third reaction processes. This difference may be a consequence of a difference in reaction temperature (388 K for SI, 333 K for SII).

The calculated $C_i(\infty)$ value in each reaction process and the $C(\infty)$ ($=C_1(\infty) + C_{2,3}(\infty)$) values may be used to evaluate the extent of contribution of each process to the overall reaction. For the SI and SII samples, the contribution of the third reaction is small (5%) but significant. However, for the SIII samples, 83% of the APS bound at equilibrium ($t = \infty$) participates in the initial reaction process and the contribution of the third process is negligibly small. The results therefore indicate that the first and second reaction processes are predominant in the overall APTS–SMBS reaction. In particular, for the SIII samples, the absence of a third reaction may be regarded as a consequence of the larger pore size.

Reaction mechanism

Figure 6 shows plots of C(APS) against $C((-O)_4Si)$ for the SI, SII and SIII samples. When we consider the accuracy of the C(APS) and $C((-O)_4Si)$ values, it is clear that the plots for the SI and SII samples consist of three linear portions, a, b and c, which correspond to the first, second and third reaction processes, respectively. For the SIII samples, only two linear portions a and b are seen and these correspond well to the initial and second reaction processes, respectively. Since the SII and SIII samples were prepared at the same temperature (333 K), the marked difference in the plots may be attributed to the difference in the pore size between the two sample systems, indicating that the linear portion c is characteristic of samples with a small pore size.

If we assume that reaction between one of the three hydroxyls on an APTS molecule and one of the SMBS-hydroxyls produces one molecule of an $(-O)_4Si$ species, then the slope of a C(APS) vs. $C((-O)_4Si)$ plot should be unity. However, each of the three linear portions has a different slope, indicating different numbers of APTS molecules participating in the conversion of $(-O)_3SiOH \rightarrow (-O)_4Si$. The difference is strongly dependent upon reaction time and on the nature of the three reaction processes. The relationship between the values of C(APS) and $C((-O)_4Si)$ provides significant information on the APTS–SMBS reaction, since the average concentration of APTS which has participated in the $(-O)_3SiOH$ to $(-O)_4Si$ reaction may be evaluated from the slope of the plots.

For the SI sample system (Fig. 6[A]), the slope of the first linear portion a (3.7) is greater than that of the second portion and its magnitude implies that approximately three to four APTS molecules participate in the $(-O)_3SiOH$ to $(-O)_4Si$ reaction. A similar conclusion may be made from slope a in the plot for the SII samples (Fig. 6[B]). However, it should be noted that the slopes of the a portions for the three sample systems are different from each other and that slope a for SIII (27.1) is considerably larger than those for SI (3.7) and SII (3.0). We may assume that this difference reflects the mechanism of an initial reaction process, as described below.

In the initial reaction process, when APTS molecules react with hydroxyl groups on SMBS particles, polymerization occurs simultaneously between unreacted APTS

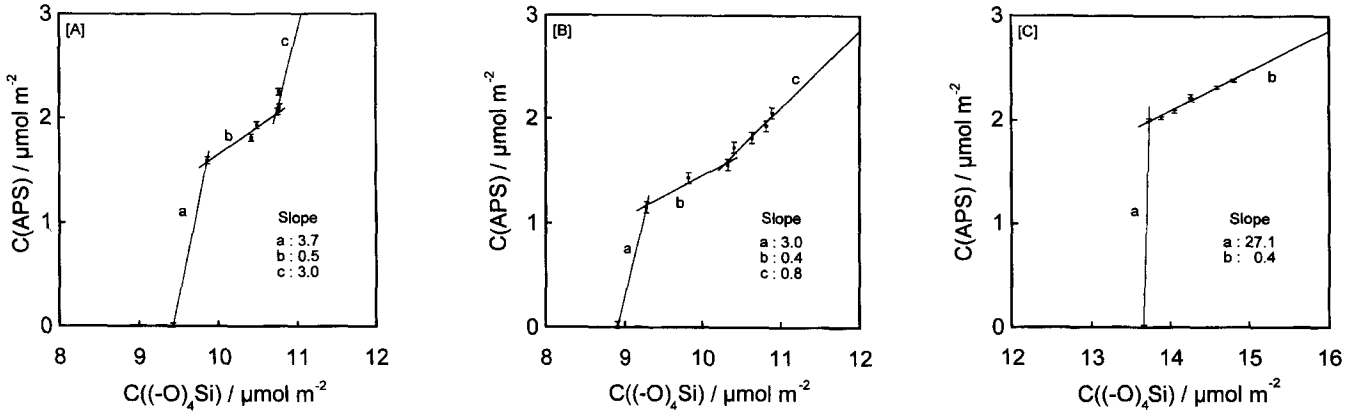

Fig. 6 Plots of C(APS) against C(($-O)_4$Si) for the three sample systems ([A]: SI, [B]: SII and [C]: SIII)

molecules and bound APS moieties. The degree of polymerization will be reflected in the value of slope a and, moreover, will depend on the pore size of an SMBS particle. For the SI and SII samples with a smaller pore size, the degree of polymerization should therefore be smaller than that for the SIII samples. However, the larger pore size of an SMBS particle should promote polymerization (see below), leading to a pronounced increase in slope a for the SIII sample. The smaller difference in the a-slopes observed for the SI and SII samples is probably due only to the effect of temperature, rather than pore size. Since unreacted APTS-molecules are limited in number, polymerization will terminate. Thus, 80% of the total quantity of APS bound at the time of first sampling (60 s) may be consumed by polymerization or oligomerization.

Caravajal et al. [20] have proposed that the amount of water involved in the silane reaction system is the critical factor in the process of polymerization. Therefore, in the second reaction process, further condensation between bound APS moieties (or among APS oligomers or APS polymers) and SMBS–hydroxyls, probably predominates. However, since this reaction process does not contribute to an increase in APS-concentration on the surface of SMBS, the slope of the linear portion b should approach zero, as observed. When the bound APS moieties react with the SMBS–hydroxyls, the unreacted hydroxyl groups of the APS moieties may be sterically hindered, leading to the observation of a higher activation energy in the second process.

We may discuss the effect of pore size on the reaction process in detail. In particular, the observation that slope a for the SIII samples (27.1) is approximately ten times that for the SII samples may be ascribed to the larger pore size of the relevant SMBS particle. For the SMBS particles used for preparation of the SI and SII samples, the average pore size (5.5 and 8.1 nm) of a particle is four to five times that (1.5 nm) of the extended form of an APTS molecule. Such a small pore size would probably prevent polymerization of APTS molecules on the silica surface and bring about an increase in the population of oligomers. Conversely, for the SIII samples, in which the SMBS particles have an average pore size of 11.6 nm, further polymerization of APTS molecules may possibly occur within the interior pore space, which will be large enough to accommodate oligomerized APTS molecules and provide extra space for their diffusion toward the pore interior and further condensation. The extremely large slope of linear portion a for the SIII samples may indicate that polymerization of APTS molecules has occurred on the surface by the time of first sampling (60 s). We may conclude that the magnitude of slope a reflects the degree of polymerization of APTS in the reaction process.

Thus, the average pore size (11.6 nm) of the SIII samples may be close to the limit of the pore size in which polymerization of APTS molecules is possible, leading to the assumption that polymerization does not occur within a pore space of diameter smaller than 8.1 nm. In this present study, we emphasize that the effect of higher temperature was examined for the SI samples on the basis of this assumption. The larger slope c in the plots for the SI samples compared with that for the SII samples may be due to the effect of this higher temperature. This result implies that a higher temperature promotes the third reaction process, as discussed below.

The initial and second reaction processes result in formation of networks of cross-linked APS oligomers (or polymers) bound on the SMBS particles. Unreacted hydroxyl groups of bound APS moieties probably still remain in the APS networks, and unreacted APTS

molecules will also be incorporated into the networks. They may cause a further condensation reaction with unreacted SMBS hydroxyls, thus constituting the third process. However, unreacted hydroxyls of bound APS moieties incorporated into the networks are likely to be extremely sensitive to steric hindrance.

Conclusion

Three sample systems were prepared by sequentially sampling the substrate from the reaction vessel at various time intervals and the rate of the APTS–silica gel reaction was monitored. The concentrations of bound APS and the corrected ^{29}Si signal intensities of an $(-O)_4Si$ species were found to be dependent upon reaction time, reflecting the rate of the APTS–silica gel reaction. Kinetic analyses of elemental analysis data suggested that the reaction of APTS and silica gel was followed by competition between a slower second reaction and a much slower third reaction. Rate constants for each reaction process have been obtained for each of the three sample systems.

The ^{29}Si NMR results show conclusively that conversion of $(-O)_3SiOH$ to $(-O)_4Si$ is the dominant contributor to the second reaction process. Identification of a correlation between C(APS) and $C((-O)_4Si)$ led to a discussion of the concentration of APTS which could participate in the conversion of $(-O)_3SiOH$ to $(-O)_4Si$.

The effect of pore size on the reaction mechanism may be summarized as follows. A small pore size effectively interrupts polymerization of APTS molecules on the silica surface and brings about an increase in the population of oligomers, while a larger pore size makes it possible for APTS molecules to polymerize.

References

1. (a) Hockey JA (1965) Chem Ind (London) 57–63; (b) Arkles B (1977) Chemtech 7:766–778
2. Davydov VY, Kiselev AV, Zhuravlev LT (1960) Trans Faraday Soc 60:2254–2264
3. Snyder LR, Ward JW (1966) J Phys Chem 70:3941–3952
4. Hair ML, Hertl W (1969) J Chem Phys 73:2372–2378
5. Armistead CG, Tyler AJ, Hambleton FH, Mitchell SA, Hockey JA (1969) J Phys Chem 73:3947–3952
6. (a) Tripp CP, Hair ML (1991) Langmuir 7:923–927; (b) Tripp CP, Hair ML (1993) J Phys Chem 97:5693–5698
7. Morrow BA, McFarian AJ (1992) J Phys Chem 96:1395–1400
8. Van Der Voort P, Gillis-D'Hamers I, Vrancken KC, Vansant EF (1991) J Chem Soc Faraday Trans 87: 3899–3905
9. Vrancken KC, Van Der Voort P, Gillis-D'Hamers I, Vansant EF, Grobet JP (1992) J Chem Soc Faraday Trans 88: 3197–3200
10. Vrancken KC, Coster LD, Van Der Voort P, Grobet JP, Vansant EF (1995) J Colloid Interface Sci 170:71–77
11. Morrow BA, Cody IA, Lee LSM (1976) J Phys Chem 80:2761–2767
12. Chiang C-H, Ishida H, Koenig JL (1980) J Colloid Interface Sci 74:396–404
13. Murthy Shreedhara RS, Leyden DE (1986) Anal Chem 58:1228–1233
14. Murthy Shreedhara RS, Blitz JP, Leiden DE (1986) Anal Chem 58:3167–3172
15. Moses PR, Wier LM, Lennos JC, Finklea HO, Lenhard JR, Murray RW (1978) Anal Chem 50:576–585
16. DiBencdetfo AT, Scola DA (1978) J Colloid Interface Sci 64:480–500
17. Cain JF, Sacher E (1978) J Colloid Interface Sci 67:538–540
18. Maciel GE, Sindorf DW (1980) J Am Chem Soc 102:7606–7607
19. Sindorf DW, Maciel GE (1983) J Am Chem Soc 105:1487–1493
20. Caravajal SG, Leyden DE, Quinting GR, Maciel GE (1988) Anal Chem 60:1776–1791
21. Furusawa K (1996) Colloid Science IV; Tokyo Kagaku Dojin Inc. Tokyo, Chapter 10, 266–267
22. Kaneko K (1996) Colloid Science IV; Tokyo Kagaku Dojin Inc. Tokyo, Chapter 11, 313
23. Shimizu I, Yoshino A, Okabayashi H, Taga K, Nishio E, O'Connor CJ (1996) J Chem Soc Faraday Trans, submitted
24. Kuester JL (1973) Optimization Techniques with Fortran. McGraw-Hill, New York, Ch 6, pp 203–271